Excited-State Processes in Phycocyanobilin Studied by Femtosecond Spectroscopy[†]

Mark Bischoff,[‡] Gudrun Hermann,*,[§] Sabine Rentsch,[‡] Dietmar Strehlow,[§] Stefan Winter,[‖] and Haik Chosrowjan[⊥]

Institute for Optics and Quantumelectronics, Friedrich-Schiller-University Jena, Max-Wien Platz 1, D-07743 Jena, Germany, Institute of Biochemistry and Biophysics, Friedrich-Schiller-University Jena, Philosophenweg 12, D-07743 Jena, Germany, Institute of Molecular Biotechnology, Beutenbergstrasse 11, D-07745 Jena, Germany, and Institute for Laser Technology, Utsubo-Hommachi 1-8-4, Osaka 550-0004, Japan

The light-induced photoprocesses of phycocyanobilin were studied by femtosecond spectroscopy. After excitation with 100 fs pulses at 610 nm the transient absorption spectra were measured throughout the visible region as a function of time. Following excitation of phycocyanobilin bleaching of the initial ground-state absorption and broad excited-state absorptions located at the shortwave and longwave sides of the bleaching region were observed. The decay of both bleaching and the excited-state absorptions was accompanied by the build-up of a comparatively long-living transient absorption between 600 and 750 nm, which is ascribed to the formation of a photoproduct. On the basis of a global analysis the observed transient absorption changes are well described by three exponential components with lifetimes in the range of a few picoseconds ($\tau_1 \sim$ 3 ps), some tens of picoseconds ($\tau_2 \sim 30-50$ ps) and some hundreds of picoseconds ($\tau_3 \sim 350-600$ ps) with the exact values depending on the solvent used for the dissolution of phycocyanobilin. The two fast components (τ_1 and τ_2) can be attributed to the relaxation of two different excited states populated with excitation, while the longer-lived component (τ_3) is associated with the decay of the photoproduct. A possible kinetic model that explains the mechanism of the light-induced relaxation processes in phycocyanobilin is presented.

Introduction

Open-chain tetrapyrrole compounds play an important role as chromophores in biological photoreceptors. Both phytochrome, the photomorphogenic pigment of green plants, and phycobiliproteins, the light-harvesting pigments in the photosynthetic apparatus of some algae, contain a tetrapyrrolic chromophore that is covalently bonded by a thioether linkage to a protein moiety. The biological action of these photoreceptors is based on the photophysical and photochemical processes occurring after the absorption of light in their bilindion chromophores. In view of this fact, studies on the photochemistry and photophysics of tetrapyrrole compounds, the structure of which is related to the chromophores in the photoreceptors, have gained increasing attention in recent years.[1−8] It is expected that such studies contribute to a better understanding of the more complex photoprocesses in the native photoreceptors. In addition, they might provide information on how the protein moiety influences the energetic and photochemical properties of the bound chromophore.

Our own investigations are concerned with the characterization of the primary photoprocesses in phytochrome, the photoreceptor for a variety of morphogenic and developmental processes in plants. Phytochrome exists in two different photointerconvertible forms, a red light-absorbing form, Pr, and a far-red light-absorbing form, Pfr. Upon photoconversion of Pr to Pfr phytochrome becomes biologically active (for more details see refs 9−12).

$$\text{Pr} \underset{730\,\text{nm}}{\overset{666\,\text{nm}}{\rightleftharpoons}} \text{Pfr} \rightarrow \text{biological response}$$
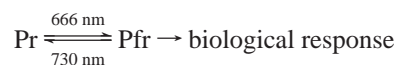
Despite considerable efforts the molecular and kinetic mechanism of this phototransformation is not yet well understood. To gain further insight into the phototransformation mechanism we have investigated the primary events following photon absorption in red light-absorbing and far-red light-absorbing phytochrome by use of picosecond and femtosecond spectroscopy.[13−17]

In the present paper, we have studied the primary events occurring in phycocyanobilin after light absorption. Phycocyanobilin is considered to be an adequate model of the Pr chromophore because its chemical structure differs from the Pr chromophore only in the side chain at C-18, which is an ethyl group in phycocyanobilin and a vinyl group in the Pr chromophore (Figure 1).

From studies such as the one presented here we, therefore, hope to obtain further information that could help to understand the complex mechanism of the light-induced processes in the Pr form of phytochrome. To follow this strategy, we have examined the solvent dependence of the excited-state properties of phycocyanobilin in a solvent system consisting of primary alcohols of different chain lengths. By including different solvents, we should address the question whether a specific solvent environment allows for a certain control of the light-induced processes.

Excited-State Processes in Phycocyanobilin

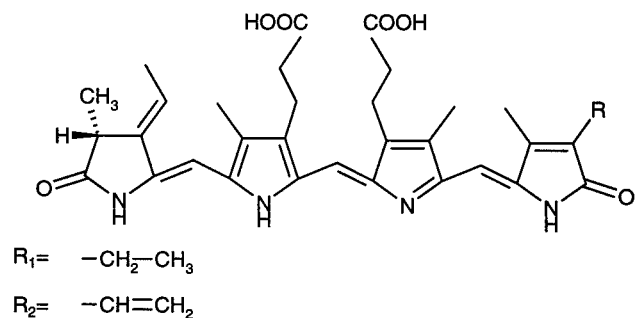*J. Phys. Chem. B, Vol. 104, No. 8, 2000* **1811**

Figure 1. Structural formula of the chromophore of phytochrome (R_1), phytochromobilin, and phycocyanobilin (R_2).

The excited-state behavior of phycocyanobilin was probed in the different alcohols by using femtosecond time-resolved spectroscopy. The obtained spectral data were analyzed by a global fit algorithm and then fitted to an adequate kinetic model. A possible kinetic mechanism that resulted from this analysis is discussed.

This report describes the first experimental investigation of phycocyanobilin using femtosecond spectroscopy.

Material and Methods

Preparation of Phycocyanobilin. Phycocyanobilin was isolated from the cyanobacterium *Spirulina geitleri* using a modification of the methods reported by Kufer and Scheer[18] and Terry et al.[19]

In a first step the cells of *Sp. geitleri* were broken and repeatedly extracted with methanol in order to remove the chlorophyll. Phycocyanobilin was cleaved from phycocyanin by boiling the remaining blue pellet in methanol under reflux with stirring for 16 h in an argon atmosphere. The resulting supernatant was evaporated and the dry residue again dissolved in methanol. In this solution, proteins were precipitated by the addition of diethyl ether and removed by filtration. Phycocyanobilin was extracted into a solution of 0.1 N HCl. The acidic solution was then adjusted to pH 6.0 with sodium acetate, and phycocyanobilin was reextracted into diethyl ether. The diethyl ether phase was concentrated to dryness by rotary evaporation, and the residue was taken up in methanol. The resulting blue solution was fractionated by column chromatography on hydroxyapatit. The column was previously equilibrated with 10 mM potassium phosphate buffer pH 8.0 containing 10% methanol. After the sample was loaded, the column was eluted with the same buffer. The material separated into a green, violet, and a faint blue band. After the elution of these bands phycocyanobilin was desorbed using a 100 mM potassium buffer at pH 8.0.

The chromatography was monitored at 620 nm and the fractions obtained were characterized spectrophotometrically. Fractions corresponding to a specific absorbance ratio (A_{365}/A_{610}) of ≥ 3.0 were pooled and washed twice with 1/4 volumes of diethyl ether. After acidification of the solution with 0.0025 volumes of glacial acetic acid, phycocyanobilin was extracted into chloroform. The blue chloroform solution was thoroughly washed with water and evaporated to dryness. The residue was again taken up in chloroform containing 3% methanol and precipitated by addition of three volumes of hexane. Following centrifugation, the resulting solid was dried with a slow stream of argon, further dried by pumping on a vacuum line, and stored at room temperature in the dark in evacuated glass vessels.

For the time-resolved measurements samples of phycocyanobilin were freshly diluted in the desired solvent to give an optical density of ~ 0.7 at 610 nm and degassed with argon. Furthermore, triethylamine was added to a final concentration of 0.3% in order to ensure that phycocyanobilin was present in its unprotonated form. During the measurements the samples were pumped through a flow cuvette. The flow rate was calculated so that under the experimental conditions used each laser pulse excited a fresh portion of the sample. After each measurement it was checked that the absorption spectrum of the sample remained unchanged in comparison with the initial spectrum.

Instrumentation and Measuring Procedure. *Absorption Measurements.* The laser used in the femtosecond spectrometer was a colliding pulse mode-locked dye laser with a four-stage dye amplifier, as described previously.[15,20] Amplified pulses of the CPM laser at 610 nm served as pump pulses. The typical photon fluence at the entrance of the cuvette was $\sim 5 \times 10^{15}$ cm^{-2}. The probe beam was a femtosecond white light continuum generated in a sapphire. The pump pulses exhibited a 100 fs pulse width. The pump and probe pulses were polarized in parallel. The chirp of the white light continuum was numerically compensated to <0.2 fs/nm. The time resolution thus obtained in the spectral region between 450 and 850 nm was ~ 200 fs. The probe light transmitted through the sample was detected by a CCD camera after passing through a spetrometer. The spectral resolution of the measurements was better than 5 nm.

To monitor the time evolution of the absorption changes, the probe pulse was delayed step by step with respect to the excitation pulse by means of a variable optical delay line. By averaging over at least 50 laser shots at each delay time, statistical fluctuations of the excitation and probe pulses were compensated.

Absorption changes were measured as the difference in optical densities (ΔA) with and without excitation. The obtained kinetic data were analyzed in terms of a sum of exponentials by a scanning global fit analysis.

Fluorescence Measurements. Time-resolved decays of the fluorescence emission were measured using a picosecond diode laser (PicoQuant GmbH, Berlin) for fluorescence excitation. The laser having a wavelength of 635 nm was operated at a repetition rate of 2 MHz. The pulse width at half-maximum amounted to 80 ps. After having passed a polarizer, the vertically polarized excitation light was focused onto the sample flow cell, which was placed at an angle of 45° relative to the exciting light beam. Fluorescence light was collected by collimating optics and passed through a cutoff filter (cutoff wavelength 650 nm) for separation from the excitation pulses. The emission polarizer was set to the magic angle (54.7° relative to the polarization of the exciting light) in order to avoid anisotropy effects occurring in larger biomolecules on the time scale $> 10^{-10}$ s. Fluorescence light was focused onto the entrance slit of a polychromator being part of the streak camera system C4774 (Hamamatsu), which allows for time-resolved acquisition of fluorescence spectra. The measured emission $I(t)$ must be described by a sum of exponential functions being convoluted with the impulse response function $F(t)$ of the detection system.

$$I(t) = I_{bg} + \sum_{j=1}^{n} \alpha_j e^{-t/\tau_j} F(t) \qquad (1)$$

In this equation τ_j denotes the fluorescence decay time of the *j*th component and α_j the corresponding amplitude. I_{bg} accounts for the constant background due to straylight. The data measured
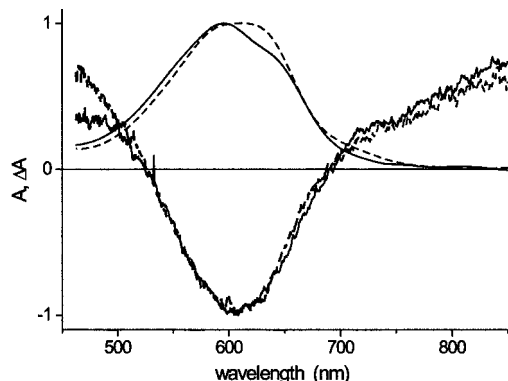
Figure 2. (Bottom panel) absorption difference spectra (ΔA spectra) of phycocyanobilin in methanol (---) and *n*-octanol (—) measured immediately after the 610 nm pump pulse has passed the sample. (Top panel) stationary absorption spectra of phycocyanobilin in methanol (---) and *n*-octanol (—). The spectra shown are normalized with a value of 1 at their peak maximum. The measurements were carried out at 293 K.

for $I(t)$ were fitted according to eq 1 using a least-squares algorithm, allowing for deconvolution with the instrument response function $F(t)$. The parameters I_{bg}, τ_j, and α_j were varied to obtain the optimum fit, which was indicated by a minimum of χ^2.

Fluorescence Up-Conversion Measurements. The fluorescence up-conversion spectrometer is described in detail by Chosrowjan et al.[21] The laser system used as light source was an Ar$^+$ laser pumped Ti:sapphire tunable laser (Mira 900, Coherent). The pulses were typically 100 fs fwhm in duration, 700 mW in energy and were dumped at a repetition rate of 76 MHz. The second harmonic was generated in a 0.2 mm BBO crystal and focused onto the sample in a 1 mm sample cell to excite the fluorescence. The fluorescence and the residual fundamental laser pulse were then focused in a 0.4 mm BBO crystal (type I) to create the up-converted signal at the sum frequency. After passing through an appropriate filter and a grating monochromator, the fluorescence was detected by a photon counting system (Hamamatsu). For the estimation of the fluorescence lifetimes the experimentally measured decay was fit to a sum of exponentials including a constant term. The constant term was added to simulate a long-lived fluorescence component, the lifetime of which cannot be determined in the time window of the femtosecond measurements.

Results

The excited-state dynamics and solvent response of the initial photoprocesses in phycocyanobilin were probed in methanol, *n*-propanol, and *n*-octanol. Phycocyanobilin was excited with 610 nm pulses of 100 fs duration, and the transient absorption changes were measured by a pump—probe technique using a broadband white light continuum as the probing light pulse. For reasons of clarity, the experimental data obtained with methanol and *n*-octanol are presented in full detail while those with *n*-propanol are only given as final results of the kinetic analysis.

Figure 2 (bottom panel) shows the absorption difference spectra ($\Delta A(\lambda)$) of phycocyanobilin in methanol and *n*-octanol as solvent measured at a delay time of 100 fs. The top panel of Figure 2 shows the stationary absorption spectrum of phycocyanobilin (referred to as *stationary spectrum* in the following) in the two solvents for comparison. As can be seen, bleaching of the initial ground-state absorption occurs immediately with excitation. In parallel with ground-state bleaching, positive transient absorption changes appear at the shortwave and
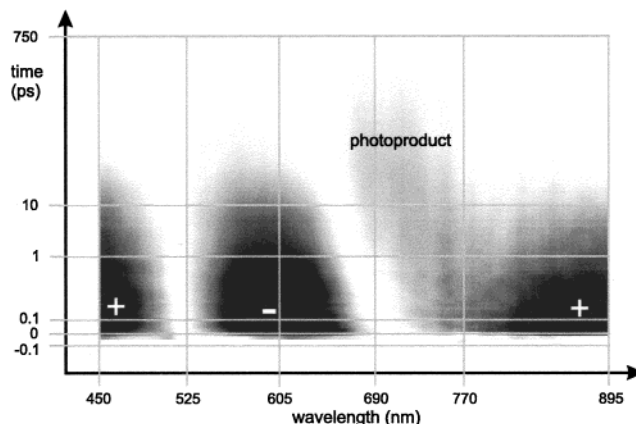

Figure 3. Density plot of the transient absorption changes (ΔA) as a function of wavelength and delay time obtained after excitation of phycocyanobilin with 100 fs pulses at 610 nm. The absolute value of ΔA is the greater, the deeper the darkening is. Phycocyanobilin used in the measurements was dissolved in methanol. The density plot for *n*-octanol as solvent is qualitatively similar to that for methanol as solvent and therefore not shown here.

longwave sides of the bleaching band. These obviously arise from the initially excited state(s) and can be attributed to excited-state absorptions. The bleaching band looks similar to the inverted stationary absorption band apart from the fact that it displays a slightly narrowed spectral shape. This is due to the positive transient absorptions that override the bleaching at its short and long wavelength tails. The similarity between the bleaching and stationary absorption band suggests that the negative absorption changes are mostly due to ground-state depletion and less to stimulated emission. The spectra measured in methanol and *n*-octanol are nearly identical. There are only small differences in the shortwave region <500 nm.

Figure 3 depicts the observed transient absorption changes in a density plot. It shows that excitation first results in an initial bleaching of the ground-state absorption, which is accompanied by the appearance of positive transient absorption changes flanking the bleaching region at the shortwave and longwave edges. While the latter absorption changes decline, another positive transient absorption appears between 600 and 750 nm. This transient absorption persists for periods beyond some hundreds of picoseconds. On the basis of its comparatively long lifetime, we assign this transient absorption to the formation of a product species.

Figure 4 reveals the transient absorption changes as a function of time for four selected wavelength regions. At 565—590 nm the negative absorption changes reflect mainly bleaching and recovery of the initial ground-state absorption. This follows from the similarity between the bleaching and the stationary absorption spectrum (Figure 2). Bleaching reaches a maximum value upon excitation and decays after that toward zero on a comparatively long time scale. At 790—815 and 475—500 nm positive absorption changes can be observed during excitation, which then undergo decay over the next tens of picoseconds. At 645—670 nm an initial bleaching takes place first, which is supplanted within several picoseconds by a positive transient absorption. For reasons mentioned above, this positive absorption most probably reflects the formation of a product state.

For a kinetic analysis the transient absorption changes were fitted to a sum of exponential functions using a global fit approach. On the basis of the global analysis the absorption changes are composed of contributions from three exponential components, one with a lifetime of a few picoseconds, another with some tens of picoseconds and a third with some hundreds
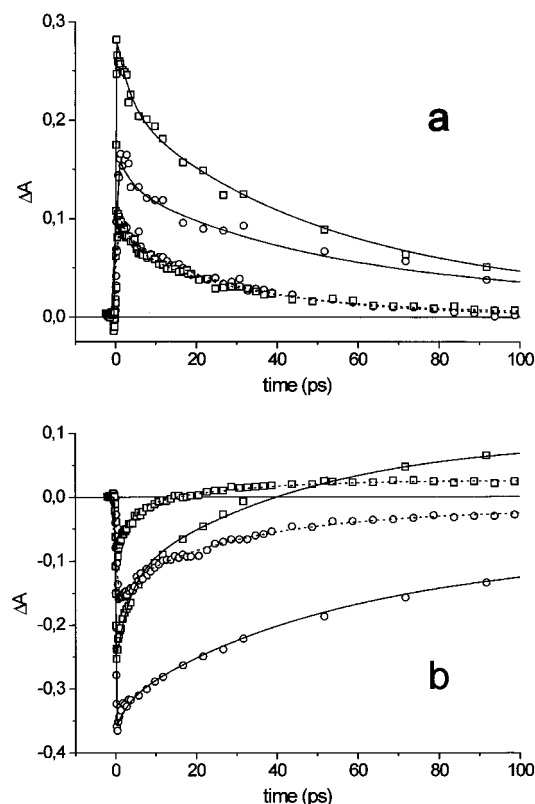
Excited-State Processes in Phycocyanobilin

J. Phys. Chem. B, Vol. 104, No. 8, 2000 **1813**

Figure 4. Kinetics of the transient absorption changes ($\Delta A(t)$) observed at selected probe wavelength regions. (a) Wavelength regions 790–815 nm (squares) and 475–500 nm (circles): (---) methanol as solvent; (—) *n*-octanol as solvent. (b) Wavelength regions 565–590 nm (circles) and 645–670 nm (squares): (---) methanol as solvent; (—) *n*-octanol as solvent. The squares and circles indicate the experimentally measured data, and the solid and dashed lines, respectively, represent the calculated functions obtained from the best fit parameters of a global data analysis. The estimated decay times are as follows: $\tau_1 = 3.2 \pm 1$ ps, $\tau_2 = 30 \pm 8$ ps, $\tau_3 = 350 \pm 100$ ps for methanol as solvent and $\tau_1 = 3.5 \pm 1$ ps, $\tau_2 = 50 \pm 10$ ps, $\tau_3 = 600 \pm 100$ ps for *n*-octanol as solvent.

TABLE 1: Decay Times (ps) of the Relaxation Processes in Excited Phycocyanobilin Measured in Different Alcoholic Solvents[a]

solvent	τ_1	τ_2	τ_3
methanol	3.2 ± 1	30 ± 8	350 ± 100
propanol	3.2 ± 1	48 ± 15	400 ± 150
n-octanol	3.5 ± 1	50 ± 10	600 ± 100

[a] The decay times were obtained from a triexponential fit using a global fit approach.

of picoseconds. The exact values obtained for these lifetimes are listed in Table 1. They are strongly dependent on the alcohol used as solvent except in the value of τ_1, which is only little affected as compared to τ_2 and τ_3. Furthermore, the amplitudes of the lifetime components vary considerably with wavelength. Thus, the decay of the excited-state absorptions at 790–815 nm is well described by the short- and intermediate-component lifetimes, τ_1 and τ_2, while the longest-component lifetime, τ_3 (aside from the short and intermediate ones), occurs in the decay of the bleaching and in the decay of the absorption changes at 645–675 nm. Figure 5 shows the amplitudes estimated from the triexponential fits for the individual decay components in dependence on the probe wavelength (decay-associated spectra).

Additionally, to facilitate the analysis of the primary processes in excited phycocyanobilin, time-resolved fluorescence measurements were carried out. Figure 6 depicts the fluorescence
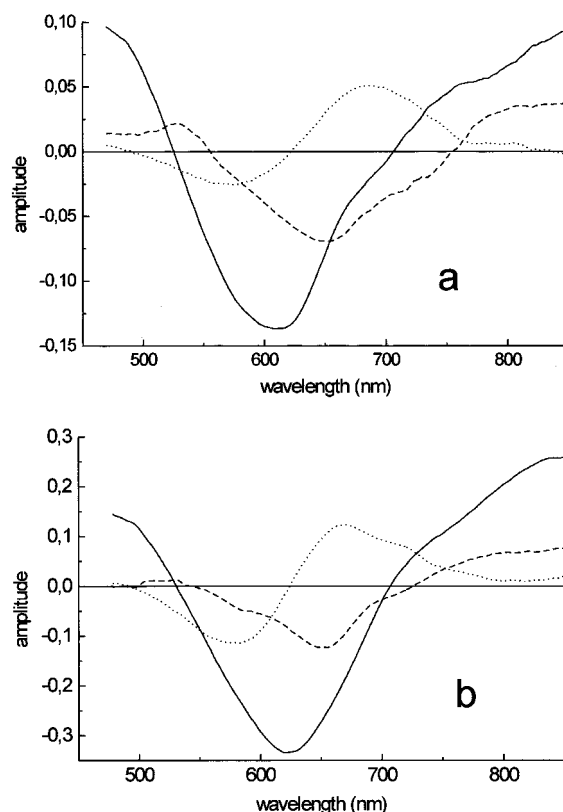

Figure 5. Decay-associated spectra of the components in the triexponential fits: (a) spectra for the fast 3.2 ps component (---), the intermediate 30 ps component (—), and the slow 350 ps component (···) in methanol as solvent; (b) corresponding spectra for the 3.5 ps component (---), the 50 ps component (—), and the 600 ps component (···) in *n*-octanol as solvent.
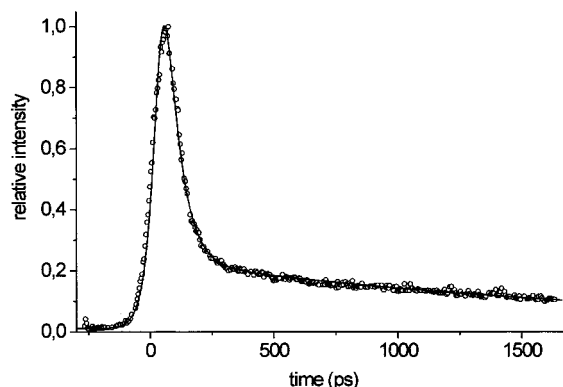

Figure 6. Fluorescence decay curve of phycocyanobilin dissolved in methanol after excitation at 635 nm. The measured decay (circles) and the decay function calculated from the best fit parameters are shown. The estimated fluorescence lifetimes are as follows: $\tau_1 = 38$ ps and $\tau_2 = 1.6$ ns.

decay of phycocyanobilin in methanol after excitation with 80 ps pulses at 635 nm. The fluorescence decays are well fitted to double-exponential decays using a deconvolution method. The main decay component with the largest relative amplitude (>90%) has a lifetime of 38 ps. The other, which makes the minor contribution to the overall decay (<10%) has a lifetime of 1.6 ns. By taking into account the considerably longer pulse duration of the exciting pulses in the fluorescence experiments, it becomes clear that the fast kinetic component (τ_1) detected in the absorption measurements cannot be resolved in the fluorescence experiments. However, it seems likely that the 38 ps fluorescence decay component corresponds, within experi-
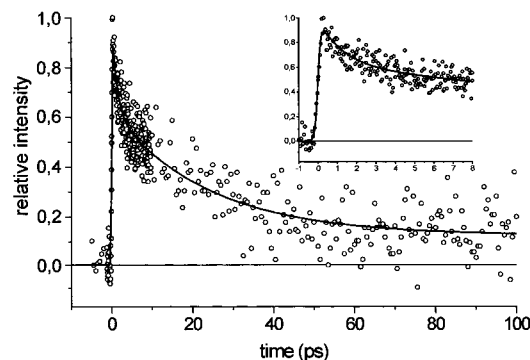
Figure 7. Fluorescence decay of phycocyanobilin dissolved in methanol as measured by the up-conversion technique. The inset displays the decay within the first 8 ps after excitation. The measured decay (circles) and the fitted decay curve (solid line) obtained from the best fit parameters are shown. The fluorescence lifetimes estimated from a biexponential fit including a constant term are as follows $\tau_1 = 2 \pm 0.8$ ps and $\tau_2 = 24 \pm 10$ ps. The constant term takes the existence of a long lifetime component (>1 ns) into account.
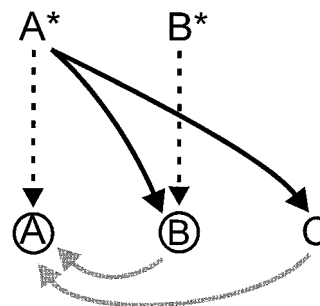

Figure 8. Kinetic scheme proposed for the light-induced processes following femtosecond excitation of phycocyanobilin. The dark arrows indicate the primary photoreaction, dashed arrows indicate internal conversion to the ground state, and gray arrows indicate the back-reaction of the photoproducts. The species enclosed by the circles are assumed to be excited by the pump pulses used in the femtosecond measurements.

mental error, to the intermediate kinetic component (τ_2) observed in the absorption measurements. Thus, it can be suggested that this component is fluorescent and therefore belongs to an excited electronic state. The longer fluorescence component has no comparable counterpart in the absorption measurements. Since this component has an amplitude of only a few percent (<10%), it is possible that the accompanying absorption is below the detection limit or that the corresponding state is not populated in the absorption measurements.

To meet the requirements necessary for the resolution of a fluorescence that corresponds to the fast kinetic component (τ_1), fluorescence measurements were made by using the up-conversion technique. The decay curve as obtained by this technique is shown in Figure 7. Fitting of the fluorescence kinetics to a sum of exponentials indicates that the decay contains three components with lifetimes of 2 ± 0.8 and 24 ± 10 ps and longer than 1 ns.

The 2 ps lifetime accords well with the value of τ_1 for the fast kinetic component, as determined in the absorption measurements. It seems very likely therefore that this component represents an excited state. Moreover, the 24 ps lifetime closely matches the value of τ_2 for the intermediate component in the absorption measurements, thus providing additional proof for the assignment of this component to another excited state. The long-component lifetime (>1 ns) is required as well for a good fit, but the accurate value of this lifetime cannot be determined in the 100 ps time window of the up-conversion measurements. Most probably this component and the 1.6 ns component observed in the above fluorescence measurements are identical.

Discussion

The key features of the ΔA spectra obtained at different delay times after femtosecond excitation of phycocyanobilin can be summarized as follows. First, immediately after excitation, bleaching of the ground-state absorption takes place. Bleaching decays non single exponentially and can be resolved into three exponential components with decay times of a few picoseconds (τ_1), a few tens of picoseconds (τ_2), and a few hundreds of pico-seconds (τ_3) depending on the solvent used for the dissolution of phycocyanobilin. Second, in parallel with bleaching, positive transient absorption changes that can be ascribed to excited-state absorptions appear at the blue and red wings of the stationary absorption band. These absorptions undergo decay with relaxation times corresponding to τ_1 and τ_2. Third, the decay

of the excited-state absorptions is accompanied by the build-up of a transient absorption between 600 and 750 nm, which disappears with the time constant τ_3 in some hundreds of pico-seconds. Because of its comparatively long lifetime this absorption most probably reflects the formation of a product species.

To describe the experimental results in terms of a kinetic model, the following considerations were taken into account. The decay-associated spectrum of the long component, τ_3 (Figure 5), represents the difference spectrum between the product species and unphotolyzed phycocyanobilin. This spectrum exhibits, in addition to the photobleaching band, an absorption band that maximizes at 690 nm and overlaps in part with the stationary absorption band. From this fact it can be concluded that the product species does arise from the photo-reaction in excited phycocyanobilin and also exists as ground-state species already before excitation. Thus, it seems very likely that two different ground-state species (A and B) occur which are electronically excited into two different excited states upon light absorption. As a consequence of the subsequent relaxation processes, the one species (B) is accumulated. Further, it was taken into account that low-temperature UV−vis spectra indicate the presence of a small fraction (<10%) of still another ground-state species, C, which exhibits an absorption maximum near 710 nm (unpublished results). Because of its longwave absorp-tion maximum in relation to the 610 nm pump pulses, this species is assumed to be not excited under our experimental conditions. However, from the long red wavelength tail in the difference spectrum of the product species (Figure 5) it may be supposed that species C is also a constituent of the product absorption. For this reason, two product species, B and C, are considered generated as a result of the photoreaction of species A. On the basis of this argument, the following kinetic model is proposed (Figure 8).

The excitation at 610 nm leads to the population of two different excited states, the one (B*) with a lifetime of τ_1 (~3 ps) and the other (A*) with a lifetime of τ_2 (30−50 ps depending on the solvent). This can be concluded from the positive absorp-tion changes that appear with excitation and decay with time constants of τ_1 and τ_2. That these two decay times are associated with the relaxation of singlet excited states is corroborated by the results of the fluorescence measurements. Kinetic processes with time constants of τ_1 and τ_2 are also detected in the recovery kinetics of the bleaching, suggesting that the molecules in either excited state return directly into the ground state. However, a part of the molecules in state A* is in addition depopulated toward two transient product states, the existence of which can be deduced from the long-living transient absorption extending
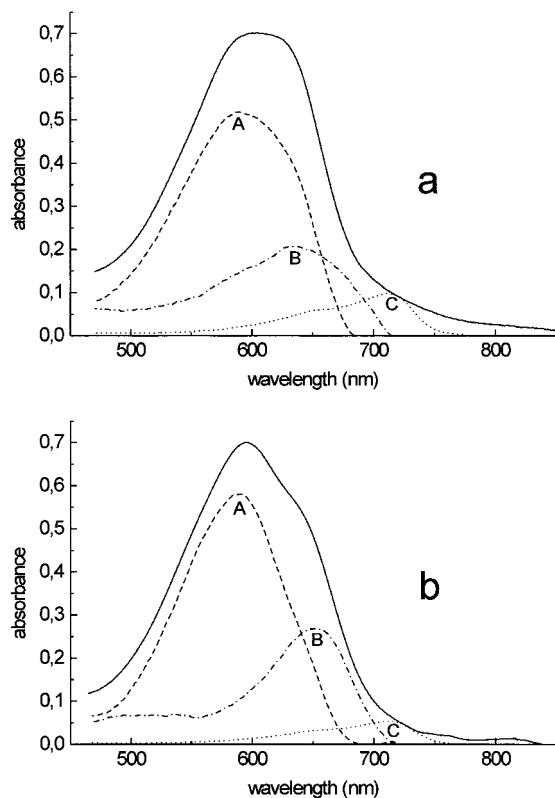
Excited-State Processes in Phycocyanobilin

J. Phys. Chem. B, Vol. 104, No. 8, 2000 **1815**

Figure 9. Absorption spectra of species A, B, and C calculated as described in the text: (a) individual absorption spectra of species A (---), B (− · −), and C (•••) in comparison with the stationary absorption spectrum of phycocyanobilin (−) in methanol as solvent; (b) corresponding spectra in *n*-octanol as solvent.

between 600 and 750 nm. The product species arising from the excited-state decay of A* are identical with species B and C present already as ground-state species in unphotolyzed phycocyanobilin but accumulating in the course of the primary photoreaction of species A. As can be judged from the product kinetics, the two product states undergo decay with the comparatively slow time constant τ_3. The decay apparently leads to the repopulation of the ground state since the same time constant is also observed in the recovery kinetics of the bleaching. After the decay of the two product states, the bleaching of the initial absorption band is fully relaxed and the resultant absorption spectrum is identical to that before excitation. This indicates that the product species B and C are obviously reconverted into species A until a thermal equilibrium of species A, B, and C is retained. The equilibrium thus reached corresponds to that of the initial steady state before excitation.

On the basis of the above kinetic model the individual absorption spectra of species A, B, and C were calculated by a global fit method. The resulting spectra are shown in Figure 9. They can be used to estimate the relative contribution of each species to the stationary absorption spectrum. The values so obtained are 68 ± 5% for species A, 25 ± 5% for species B, and 7 ± 2% for species C when methanol is used as solvent and 63 ± 5% for species A, 33 ± 5% for species B, and 4 ± 2% for species C when *n*-octanol is used as solvent.

The following criteria suggest that the proposed kinetic model provides a proper fit of the experimental ΔA spectra. First, if the absorption spectra and true rate constants calculated from the model are used for a simulation, there is very good agreement between the simulated and experimentally measured ΔA spectra. The residual spectra at different delay times are only composed of random noise within the noise level of the

experimental data. Second, the calculated absorption spectra are a smooth function of the wavelength and consist of only one main absorption maximum. Furthermore, the absorption is positive at any wavelength. If the experimental ΔA spectra were fit assuming an unbranched sequential model which allows the formation of a product species that is not identical with an essential component of the original stationary absorption band, the results obtained were less consistent.

The calculated absorption spectra (Figure 9) indicate a clear red shift of the spectra for species B and C from the spectrum for species A, which undergoes the photoreaction into species B and C. The red shift does not directly provide information on the structural changes involved in the photoreaction. However, taking into account the factors determining the spectral properties of open-chain tetrapyrroles,[22] the red shift should be associated with an extension of the conjugated π-electron system in the longitudinal dimension *x*. Considering further that, according to NMR studies,[8] species A adopts a cyclic helical conformation, the elongation of the conjugation path in dimension *x* should be brought about by a rotation about one of the formal single bonds in the exocyclic methine bridges, leading to a more extended conformation. Compared to the length in dimension *x,* the general shape of the conjugated π-electron system does not significantly change on isomerization at one of the exocyclic double bonds. We therefore assume that most of the red shift in the product absorption is due to a photoreaction that involves a single bond rotation at one of the methine bridges, yielding a more stretched arrangement of the tetrapyrrole ring system.

Another result of our measurements is the demonstration of a solvent effect on the decay times τ_2 and τ_3. When the solvent is changed from methanol via propanol to *n*-octanol, the decay times τ_2 and τ_3 become significantly longer, while little change occurs in τ_1 (Table 1). The time constant τ_2 is related to the excited-state decay of species A and τ_3 to the decay of the two product species (Figure 8). It thus seems likely that interactions between the solute and the surrounding solvent control these two relaxation processes. The series of alcoholic solvents used in the experiments differ with respect to various solvent properties such as the dielectric constant, the refractive index, and the viscosity. At present we do not know which of these properties is of prime importance for the solvent response. But supposing that the formation of the product species B and C and their reconversion into species A involves single bond rotations at the exocyclic methine bridges, as suggested above, the lengthening of τ_2 and τ_3 with increasing alcohol length might indicate a dependency on the solvent viscosity. It would be expected that molecular motions of this kind are more hindered the higher the viscosity of the surrounding solvent is.

In conclusion, our results indicate that the primary photoreaction in phycocyanobilin occurs on the time scale of a few tens of picoseconds. When the order of magnitude of this time constant is compared with the formation rate of ($\sim$32 ps)$^{-1}$ for the first photoproduct in the phototransformation of the Pr form of phytochrome,[15] a close correspondence becomes evident. It thus appears that the primary photochemical event in open-chain tetrapyrroles takes some tens of picoseconds. This reaction rate is about 2 orders of magnitude slower than that of the primary photoreactions in bacteriorhodopsin and the photosynthetic reaction centers that proceed on the <1 ps time scale.

Our results further show that the time constant τ_2 for the initial photoreaction (aside from the time constant (τ_3) for the back-reaction of the photoproducts) is solvent dependent. When again a parallel is drawn to the primary photoprocesses in phyto-

chrome, this fact suggests that solute−solvent interactions might also play a role in controlling the light-induced photoreaction. It is possible that relaxational interactions between the open-chain tetrapyrrole chromophore and the surrounding protein sites are of importance for both the rate and the selectivity of the primary photoreaction.

References and Notes

(1) Falk, H.; Grubmayr, K.; Magauer, K.; Müller, N.; Zrunek, U. *Isr. J. Chem.* **1983**, *23*, 187.

(2) Siebert, F.; Grimm, R.; Rüdiger, W.; Schmidt, G.; Scheer, H. *Eur. J. Biochem.* **1990**, *194*, 921.

(3) Braslavsky, S. E.; Schneider, D.; Heilhoff, K.; Nonell, S.; Aramendia, P. F.; Schaffner, K. *J. Am. Chem. Soc.* **1991**, *113*, 7322.

(4) Ditto, M.; Brunner, H.; Lippitsch, M. E. *Chem. Phys. Lett.* **1991**, *185*, 61.

(5) Smit, K.; Matysik, J.; Hildebrandt, P.; Mark, F. *J. Phys. Chem.* **1993**, *97*, 11887.

(6) Korkin, A.; Mark, F.; Schaffner, K.; Gorb, L.; Leszcynski, J. *J. Mol. Struct. (Theochem.)* **1996**, *388*, 121.

(7) Knipp, B.; Kneip, K.; Matysik, J.; Gärtner, W.; Hildebrandt, P.; Braslavsky, S. E.; Schaffner, K. *Chem. Eur. J.* **1997**, *3*, 363.

(8) Knipp, B.; Müller, M.; Metzler-Nolte, N.; Balaban, T. S.; Braslavsky, S. E.; Schaffner, K. *Helv. Chim. Acta* **1998**, *81*, 881.

(9) Rüdiger, W.; Thümmler, F. *Angew. Chem., Int. Ed. Engl.* **1991**, *30*, 1216.

(10) Furuya, M.; Song, P.-S. *Photomorphogenesis in Plants*, 2nd ed.; Kluwer Academic Publishers: Dordrecht, The Netherlands, 1994; p 105.

(11) Quail, P. H.; Boylan, M. T.; Parks, B. M.; Short, T. W.; Xu, Y.; Wagner, D. *Science* **1995**, *268*, 675.

(12) Quail, P. H. *Philos. Trans. R. Soc. London* **1998**, *B 353*, 1399.

(13) Lippitsch, M. E.; Hermann, G.; Brunner, H.; Müller, E.; Aussenegg, F. R. *J. Photochem. Photobiol.* **1993**, *18*, 17.

(14) Büchler, R.; Hermann, G.; Lap, D. V.; Rentsch, S. *Chem. Phys. Lett.* **1995**, *233*, 514.

(15) Rentsch, S.; Hermann, G.; Bischoff, M.; Strehlow, D.; Rentsch, M. *Photochem. Photobiol.* **1997**, *66*, 585.

(16) Rentsch, S.; Bischoff, M.; Hermann, G.; Strehlow, D. *Appl. Phys.* **1998**, *B 66*, 259.

(17) Bischoff, M.; Hermann, G.; Rentsch, S.; Strehlow, D. *J. Phys. Chem.* **1998**, *102*, 4399.

(18) Kufer, W.; Scheer, H. *Hoppe-Seyler's Z. Physiol. Chem.* **1979**, *360*, 935.

(19) Terry, M. J.; Maines, M. D.; Lagarias, J. C. *J. Biol. Chem.* **1993**, *268*, 26099.

(20) Rentsch, S.; Lap, D. V.; Helbig, M.; Grebner, D. *Exp. Techn. Phys.* **1996**, *42*, 47.

(21) Chosrowjan, H.; Mataga, N.; Nakashima, N.; Imamoto, Y.; Tokunaga, F. *Chem. Phys. Lett.* **1997**, *270*, 267.

(22) Falk, H. *The chemistry of linear oligopyrroles and bile pigments;* Springer-Verlag: New York, 1989; p 400.